Journal of Non-Crystalline Solids: X 17 (2023) 100174

Contents lists available at ScienceDirect

Journal of Non-Crystalline Solids: X

journal homepage: www.sciencedirect.com/journal/journal-of-non-crystalline-solids-x

Photoluminescence emission in arsenic sulfide nanocomposite

George Alkhalil [a,*], Julia A. Burunkova [a], Maria Stepanova [b], Andrey Veniaminov [b], Boglarka Donczo [c], Mate Szarka [c], Sandor Kokenyesi [d]

[a] Laboratory of Quantum Processes and Measurements, Centre for Chemical Engineering, ITMO University, Saint Petersburg 197101, Russia
[b] Laboratory of Hybrid nanostructures for biomedicine, Centre for Physics of nanostructures, ITMO University, Saint Petersburg 199034, Russia
[c] Institute for Nuclear Research (ATOMKI), Debrecen 4026, Hungary
[d] Department of Electrical Engineering, Debrecen University, Debrecen 4032, Hungary

ARTICLE INFO

Keywords:
Arsenic sulfide
Photoinduced structural transformations
Nanocomposite
Porous glasses
Photoluminescence

ABSTRACT

Synthesis and characterization of the optical properties of materials especially at a nanoscale, is considered as important tasks for the engineering of photonic devices and systems. In this paper we study the photoluminescence of new nanocomposite material consisting of arsenic sulfide doped in porous glasses and the effect of photoinduced structural transformations on it. The nanocomposite was obtained via chemical deposition method in which arsenic sulfide powder was dissolved in an amine solution and then clean pieces of porous glass were impregnated for 2 days in the solution. Strong photoluminescence signal was observed in the samples when excited with lasers with excitation wavelengths of 405 and 532 nm. Also, the effect of laser irradiation on the photoluminescence of the samples was studied using confocal microscope with two different operating lasers 405 and 514 nm. It was observed that laser irradiation influences photoluminescence differently depending on the irradiation wavelength.

1. Introduction

Arsenic sulfide (As_2S_3) is a chalcogenide material that possesses several unique physical and optical properties [1]. Photoinduced phenomena, such as stimulated changes of optical absorption and refraction spectra are the most special properties observed in arsenic sulfide glasses and have been widely studied [2–5]. Aside from the applications of As_2S_3 in passive devices such as optical fibers [6] and media for optical recording [7], it was recently observed that As_2S_3 also can be an excellent active medium for applications in nonlinear optics such as supercontinuum generation in the infrared region [8]. As_2S_3 photonic crystal fiber was used for broadband infrared supercontinuum generation extending from 2.5 to 15 μm [9]. Second harmonic generation was observed in thermally poled As_2S_3 glasses [10]. As_2S_3 planar waveguide was used for broadband cascaded four wave mixing [11], and in another work for correlated photon-pair generation [12].

The photoluminescence (PL) in arsenic sulfide glasses was first observed by Kolomiets' group [13], and since then it has been extensively studied by others [14–16]. Tanaka compared the PL of As—S system with its crystal form with respect to composition, temperature and excitation spectra. Tanaka [17] observed substantially different PL depending on the excitation energy relative to the bandgap of the system. The PL intensity starts to decrease when increasing the temperature over 4 K or when changing the excitation energy further from (decrease or increase) the bandgap energy. The ageing effect in air on the PL of glassy and crystalline As_2S_3 was studied by applying different excitation energies [18]. Some PL characteristics of both aged glassy and crystalline As_2S_3 were found to be as a results of oxidation process on the surface of the samples and accompanied by realgar to pararealgar transformation in the aged glassy As_2S_3. Strong PL emission was observed at room temperature in 2D- As_2S_3 with a laser excitation wavelength of 473 nm [19]. In the same work, the influence of composition on the PL spectra was studied. It was observed that As_4S_4 realgar structural units sharply quench the PL and the cyclic As_2S_2 structure is the main reason of PL in 2D- As_2S_3. Thin films of arsenic sulfide prepared by PECVD-based method shown to exhibit broad PL spectra with the maximum intensity shifts from 1.87 to 2.42 eV when changing the composition from $As_{35}S_{65}$ to $As_{55}S_{45}$ [20].

Recently, we observed a pronounced reversible photobleaching effect (a blue shift in the transmission spectrum that can be reversed by thermal treatment) in arsenic sulfide doped in porous glasses. This is an intriguing effect because it is the opposite of the effect usually observed

* Corresponding author.
E-mail address: gorg.kalel@yahoo.com (G. Alkhalil).

https://doi.org/10.1016/j.nocx.2023.100174
Received 30 November 2022; Accepted 25 February 2023
Available online 28 February 2023

for As_2S_3 bulk glasses and thin films (i.e., photodarkening.) [21]. In this article, we study the PL of arsenic sulfide doped in porous glasses and the influence of irradiating the samples on its PL.

2. Experimental

2.1. Materials

The arsenic sulfide glass As_2S_3 used in this work was obtained via direct synthesis of high-purity elements in quartz ampules. Propylamine (No. 109819, 98%) used to dissolve As_2S_3 was purchased from Sigma-Aldrich. Silica-based porous glass (PG, 6 × 10 mm, 2.5 mm thick) obtained by acid leaching of sodium borosilicate glass with the composition 7 Na_2O, 23 B_2O_3, 70 SiO_2 were used. The used PGs had an average pore size of 23 nm, and a specific surface area ranging from 10 to 300 m^2/g [21].

The PG's mass was measured before and after impregnation to define the dopant concentration (As_2S_3) in the glass. The samples studied in this work have a concentration around 2%.

3. Methods

The samples of arsenic sulfide doped porous glasses studied in this work were prepared as follows. 0.03 g As_2S_3 was dissolved in 2.5 mL propylamine, and after the complete dissolution of As_2S_3, pieces of PG were added to the solution. The PG samples were extracted from the solution after two days, left to air dry for 1 h, and then annealed at 190 °C for 2 h. After thermal treatment, the samples were transparent and brown colored.

3.1. Characterization

The obtained samples were characterized using optical spectrometry, scanning electron microscopy, Raman spectroscopy, and confocal laser microscopy.

The optical transmission spectra of the samples were measured in the visible-near infrared spectral region on a Fluorat-02-Panorama spectrofluorometer (Lumex Instruments, Saint Petersburg, Russian Federation). A DPSS laser with the emission wavelength 532 nm (KLM-532/h/100, FTI Optronic, Russian Federation) was used for irradiating the samples and for excitation when measuring their PL.

The composition of the samples was determined using scanning electron microscope (Hitachi S4300-CFE, Japan). The microscope was equipped with energy dispersive X-ray (EDX) spectroscopy measuring capability. It was used for composition measurements with a detection threshold of 0.1%.

The photoinduced transformations were investigated by measuring the Raman spectra of the samples before and after irradiation. Measurements were performed on an InVia Raman microscope (Renishaw, Wotton-under-Edge, United Kingdom) in the Raman shift range 100–700 $/cm^{-1}$ using a 785 nm laser as an excitation source.

The PL spectra were measured at room temperature employing USB4000 Spectrometers (Ocean Insight, USA) with 405 and 532 nm lasers for excitation. The effect of irradiation on the PL intensity of the samples was investigated by A confocal luminescent scanning microscope LSM-710 (Carl Zeiss Microimaging, Germany) at two excitation wavelengths; 405 and 514 nm.

4. Results and discussion

4.1. PG- As_2S_3 composition and optical properties

Compositional analysis of the impregnated PG samples was carried out on energy dispersive X-ray (EDX) spectroscope. We observed a higher As/S ratio in PG ($As_{56}S_{44}$) comparing with the ratio in $As_{40}S_{60}$ which was used for preparing the samples. Similar dependency was observed in other works [22].

Since, the prepared material exhibits photoinduced structural transformations, we investigated the effect of irradiation on its optical properties. The samples were irradiated for 45 min with green laser at an intensity of 500 mW/cm^2. The transmission spectra of the samples were measured before and after irradiation (Fig. 1) and they were employed for calculating the optical bandgap energy E_g according to Tauc method [23].

The obtained bandgap energies before and after irradiation are E_{g1} = 2.18 eV and E_{g2} = 2.45 eV, respectively. We notice that the initial bandgap energy of the samples is lower than the typical bandgap energy of As_2S_3 glass and thin films [19]. This shift can be explained by the higher As/S ratio in our samples $As_{56}S_{44}$. Similar dependency has been previously observed in several studies were the bandgap energy decreases when increasing the As/S composition [20,24].

After irradiation, we observed a pronounced blue shift in the transmission spectrum of the samples (photobleaching) accompanied with increase in the bandgap energy from 2.18 to 2.45 eV. This effect is the opposite of the effect usually observed for As_2S_3 bulk glasses and thin films (i.e., photodarkening) [25].

4.2. Raman spectra

Raman spectroscopy analysis were conducted to investigate the molecular structure, the polymorphism and the photoinduced structural transformations of the samples. Fig. 2 presents the Raman spectra of PG–As_2S_3 sample before and after irradiation.

As shown in Fig. 2 (black line), the initial PG– As_2S_3 spectrum is dominated by strong and broad band between 250 cm^{-1} and 480 cm^{-1} with its most intensive peak at 475 cm^{-1}, as well as other peaks at 218 cm^{-1} and ~150 cm^{-1}. These bands at 150 cm^{-1}, 218 cm^{-1}, 445 cm^{-1} and 475 cm^{-1} represent the exact characteristics of S—S bond-stretching vibrational modes [24]. The appearing of theses homopolar S—S bonds in arsenic sulfide glasses with high As/S ratio can be explained by the formation of separated S-rich and As-rich clusters. The broadening of the spectrum into the region between 300 cm^{-1} and 400 cm^{-1} is due to the As—S vibrational modes.

After irradiation, the bands corresponding to the homopolar bonds S—S at 150 cm^{-1} and 218 cm^{-1} disappear and several new bands appear at 188 cm^{-1}, 216 cm^{-1}, 235 cm^{-1}, 257 cm^{-1}, and 368 cm^{-1} (Fig. 2, red line), indicating the breaking of homopolar S—S bonds and the formation of As—S bonds. The new bands at 188 cm^{-1}, 216 cm^{-1}, and 367

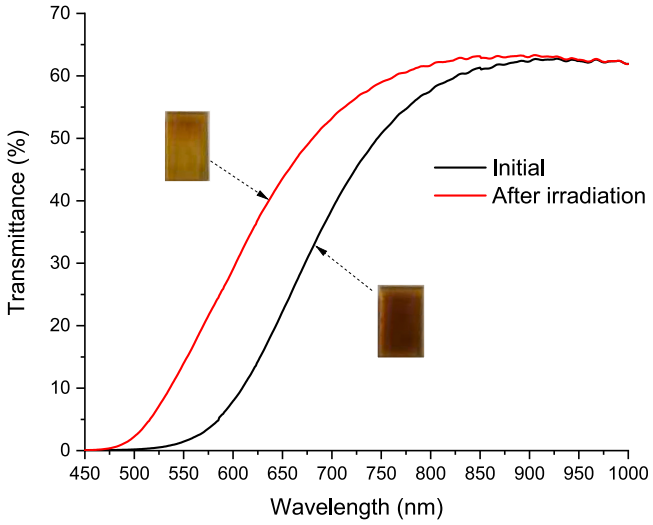

Fig. 1. Optical transmission spectra of PG–As_2S_3 before (black curve) and after irradiation (red curve). (For interpretation of the references to colour in this figure legend, the reader is referred to the web version of this article.)

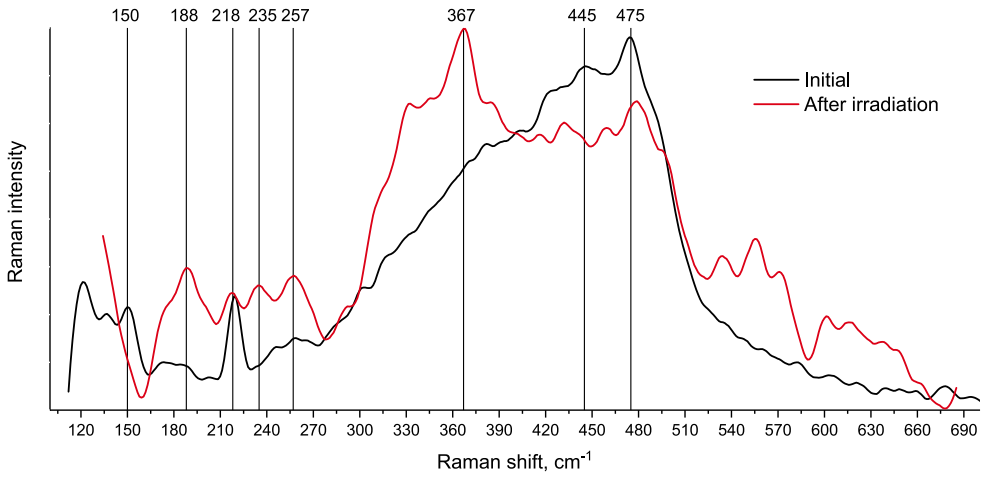

Fig. 2. Raman spectra of PG– As_2S_3 before (black curve) and after irradiation with 532 nm laser (red curve). (For interpretation of the references to colour in this figure legend, the reader is referred to the web version of this article.)

cm^{-1} are usually attributed to As—As and As—S bonds, and they appear in the Raman spectra of β-realgar-like molecules [26]. The more structured spectrum after irradiation indicates that irradiation leads to the formation of virous As—S molecular structure or nanocrystals. It is known that the bandgap energy of crystalline materials is higher than its amorphous counterpart [27]. Therefore, the increasing in the bandgap energy after irradiation also support the hypothesis of photoinduced crystallization in our samples.

An interesting fact is the appearance of the bands at 550, 600–660 cm^{-1} after irradiation. These vibrations can be assigned to the S—S bonds [28,29].

4.3. Luminescence spectra

The photoluminescence spectra of the samples were measured under excitation with 405 nm and 532 nm lasers. Since the PL spectra contain more than one Gaussian peak, we deconvoluted it to obtain more information about the PL centers. The PL spectra are presented in Fig. 3. The curves P1, P2, P3 and P4 represent the deconvoluted PL spectra and their sum is represented by curve Fit envelope. The results show a wide and intensive band at 511 nm observed when excitation $\lambda_{ex} = 405$ nm is used (Fig. 3 (a)). The deconvolution reveals four peaks centered at 446, 490, 519 and 574 nm.

The PL spectrum excited with $\lambda_{ex} = 532$ nm is dominated by a broad emission band centered around 596 nm with shoulder around 630 nm Fig. 3 (b). Three PL peaks obtained by deconvoluting this spectrum are located at 583, 616 and 660 nm.

We also investigated the influence of irradiation with different photon energies on the PL emission. To avoid any influence on the PL intensity by changing the optical element or the sample's position we conducted this investigation using confocal luminescent scanning microscopy. The PL of the samples was measured using the excitation wavelengths 405 and 514 nm before and after irradiation for five minutes with the same lasers. For irradiating the samples, laser beam with power of 1 mW was focused into 85 μm^2 area. Results are presented in Fig. 4.

It is clear that PL observed in our samples does not follow the known $E_{PL} \approx E_g/2$ rule that reflects the bulk intrinsic properties of chalcogenide glasses [13]. Note that for 405 nm excitation $E_{PL}/E_{ex} \approx 0.8 > 0.5$, and for 532 nm excitation $E_{PL}/E_{ex} \approx 0.9 > 0.5$. Moreover, it is unlikely that the obtained PL spectra is a result of As_2O_3 or As_2O_5 which can be formed by As_2S_3 oxidation, because the PL spectra of these two materials are usually characterized by distinct luminescence band at 550 nm which is absent in our case [30].

In order to compare the PL in our samples with other works we

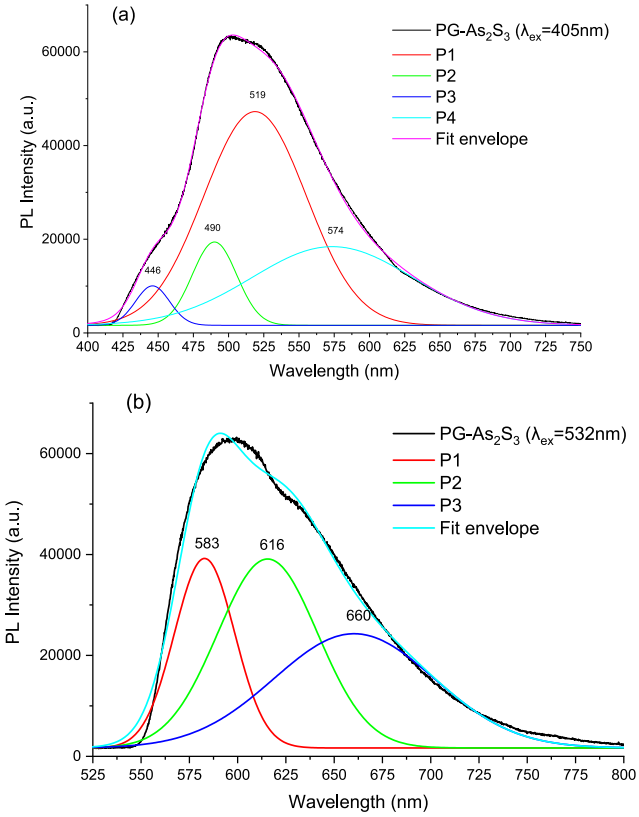

Fig. 3. Deconvoluted experimental PL spectra of PG–As_2S_3 when excited with (a) 405 nm laser and (b) 532 nm laser. Deconvoluted spectra are represented by curves P1, P2, P3 and P4. The resulted sum of the deconvoluted spectra is represented by curve fit envelope.

reviewed some works in which the $E_{PL} \approx E_g/2$ rule was violated. The PL maximum position as function of the excitation wavelength obtained for arsenic sulfide in this work and in others is presented in Fig. 5.

Fig. 5 shows that the PL energy increases when increasing the excitation energy, and it is qualitatively in the range $E_{PL}/E_{ex} \approx 0.8$–$0.9$. It should be mentioned that the PL peak emission energy in most cases is lower than the bandgap energy of samples which is about 2.4 eV. In our samples, we notice that the PL peak emission energy is close or higher than the bandgap energy. This effect can be due to the fact that the PL

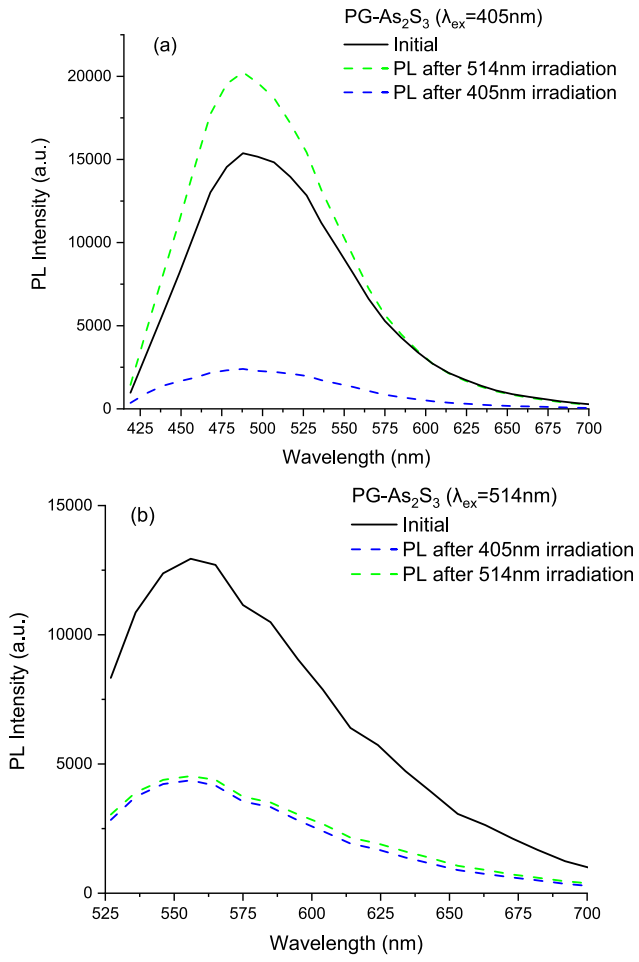

Fig. 4. Experimental PL spectra of PG– As_2S_3 when excited at (a) 405 nm and (b) 514 nm. Black solid curves represent the initial PL spectra, dashed curves represent the PL spectra after irradiation with 405 nm laser (blue curves) and with 514 nm laser (green curves). (For interpretation of the references to colour in this figure legend, the reader is referred to the web version of this article.)

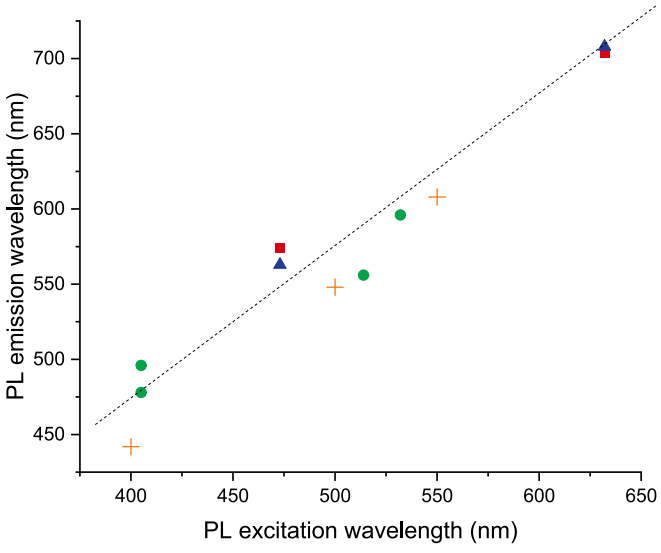

Fig. 5. The PL maximum position as function of the excitation wavelength for data obtained in this work (green circles), [33] (blue tringles), [18] (orange crosses), [19] (red squares). (For interpretation of the references to colour in this figure legend, the reader is referred to the web version of this article.)

emission from arsenic sulfide nanoparticles, rather than its bulk form, is observed [31,32].

Irradiating the samples revealed an interesting dependence of the PL spectra. The PL intensity under excitation with 405 nm laser beam decreases in the region irradiated with 405 nm laser. On the other hand, it is enhanced in the region irradiated with 514 nm laser. This can be explained by wavelength dependent photoinduced structural transformations. It was proved before that, while irradiation with bandgap energy increases the homopolar bonds concentration (As—As and S—S), irradiation with super-bandgap energy (3.06 eV or 405 nm) results in the formation of S-reach layers [34]. In the Raman spectrum after irradiation of the sample, peaks that appeared at 550, 600–660 cm^{-1}, seem to be corresponding to the S-reach layers as mentioned in [28], whose thickness at the nanoscale. In our case, as we mentioned above, irradiation with bandgap energy leads to amorphous to crystalline phase transition or nanocrystal formations, and also the formation of S-reach layers. Although it is hard to predict the exact structure and composition of the formed nanocrystals in these samples, but our measurements show that they have a relatively wide bandgap energy and exhibit PL emission in 490 nm range.

5. Conclusion

It is shown that the irradiation of arsenic sulfide doped in porous glasses significantly changes the structural configuration of arsenic sulfide. Raman studies showed that bandgap laser irradiation induces homopolar S—S bonds breaking and the formation of heteropolar As—S bonds and amorphous to crystalline phase transition. This transition is accompanied by increasing in the bandgap energy of the material. The photoluminescence of the samples was studied under excitation with different energies. Deconvoluted photoluminescence spectra revealed different emission peaks in the range of 446 to 660 nm which can be due to different molecular structures. The influence of irradiation on the photoluminescence emission intensity was also investigated. Wavelength dependent photoinduced transformation was observed. Utilizing the photoinduced changes in the obtained composite for optical recording and optimizing its optical properties makes it a promising material for the fabrication of various functional optical elements.

Declaration of Competing Interest

The authors declare that they have no known competing financial interests or personal relationships that could have appeared to influence the work reported in this paper.

Data availability

No data was used for the research described in the article.

Acknowledgements

This work was supported by the Ministry of Science and Higher Education of the Russian Federation (G.A.: Passport No. 2019-0903; M. S. and A.V.: Passport No. 2019-1080). Raman spectroscopy measurements were performed with the support of GINOP-2.3.3-15-2016-00029 project in the Institute for Nuclear Research, Debrecen, Hungary.

References

[1] H. Wang, et al., In-situ and ex-situ characterization of femtosecond laser-induced ablation on As2S3 chalcogenide glasses and advanced grating structures fabrication, Materials 12 (1) (2019), https://doi.org/10.3390/ma12010072.
[2] K. Tanaka, Reversible photoinduced change in intermolecular distance in amorphous As2S3 network, Appl. Phys. Lett. 26 (5) (1975) 243–245, https://doi.org/10.1063/1.88136.
[3] O.I. Shpotyuk, J. Kasperczyk, I.V. Kityk, Mechanism of reversible photoinduced optical effects in amorphous As2S3, J. Non-Cryst. Solids 215 (2) (1997) 218–225, https://doi.org/10.1016/S0022-3093(97)00058-6.

[4] U. Strom, T.P. Martin, Photo-induced changes in the infrared vibrational spectrum of evaporated As2S3, Solid State Commun. 29 (7) (1979) 527–530, https://doi.org/10.1016/0038-1098(79)90350-8.
[5] T.V. Moreno, et al., In situ measurements of photoexpansion in As2S3 bulk glass by atomic force microscopy, Opt. Mater. (Amst.) 94 (2019) 9–14, https://doi.org/10.1016/j.optmat.2019.05.016.
[6] V.S. Shiryaev, et al., Development of technique for preparation of As2S3 glass preforms for hollow core microstructured optical fibers, J. Optoelectron. Adv. Mater. 16 (9–10) (2014) 1020–1025.
[7] R. Tintu, K. Saurav, K. Sulakshna, V.P.N. Nampoori, P. Radhakrishnan, S. Thomas, Ge 28 Se 60 Sb 12 /PVA Composite Films for Photonic Applications, 2010.
[8] M. Kalantari, A. Karimkhani, H. Saghaei, Ultra-wide mid-IR supercontinuum generation in As2S3 photonic crystal fiber by rods filling technique, Optik 158 (2017) 142–151, https://doi.org/10.1016/j.ijleo.2017.12.014.
[9] C. Wei, H. Zhang, H. Luo, H. Shi, Y. Liu, Broadband mid-infrared supercontinuum generation using a novel selectively air-hole filled As2S5-As2S3 hybrid PCF, Optik (Stuttg) 141 (2017) 32–38, https://doi.org/10.1016/j.ijleo.2017.02.061.
[10] M. Dussauze, X. Zheng, V. Rodriguez, E. Fargin, T. Cardinal, F. Smektala, Photosensitivity and second harmonic generation in chalcogenide arsenic sulfide poled glasses, Opt. Mater. Express 2 (1) (Jan. 2012) 45–54, https://doi.org/10.1364/OME.2.000045.
[11] J. Wen, H. Fu, Broadband cascaded four-wave mixing in As2S3 chalcogenide waveguide with optical feedback and Mach–Zehnder interferometer, Mod. Phys. Lett. B 29 (21) (2015), https://doi.org/10.1142/S0217984915501158, 1550115.
[12] A.C. Judge, et al., Low Raman-noise correlated photon-pair generation in a dispersion-engineered chalcogenide As_2S_3 planar waveguide, Opt. Lett. 37 (16) (Aug. 2012) 3393–3395, https://doi.org/10.1364/OL.37.003393.
[13] B.T. Kolomiets, T.N. Mamontova, A.A. Babaev, Radiative recombination in vitreous and single crystal As2S3 and As2Se3, J. Non-Cryst. Solids 4, no. C (Apr. 1970) 289–294, https://doi.org/10.1016/0022-3093(70)90053-0.
[14] K. Murayama, H. Suzuki, T. Ninomiya, Luminescence and optically detected ESR in a-As2S3, J. Non-Cryst. Solids 35–36, no. PART 2 (Jan. 1980) 915–920, https://doi.org/10.1016/0022-3093(80)90317-8.
[15] K. Murayama, Polarization memory of photoluminescence and photoinduced optical anisotropy in chalcogenide glasses, Disord. Semicond. (1987) 185–194, https://doi.org/10.1007/978-1-4613-1841-5_22/COVER.
[16] T. Tada, T. Ninomiya, Photoluminescence from optically induced metastable states in a-As2S3, J. Non-Cryst. Solids 114 (PART 1) (Dec. 1989) 88–90, https://doi.org/10.1016/0022-3093(89)90077-X.
[17] K. Tanaka, Excitation-energy-dependent photoluminescence in glassy as–S and crystalline As2S3, Phys. Status Solidi B 250 (5) (May 2013) 988–993, https://doi.org/10.1002/PSSB.201248519.
[18] V. Mitsa, et al., Investigation of atmospheric corrosion by photon energy dependent luminescence and Raman spectroscopy in aged and freshly fractured g-,c-As2S3 with photosensitive realgar inclusions, J. Non-Cryst. Solids 453 (Dec. 2016) 23–27, https://doi.org/10.1016/J.JNONCRYSOL.2016.09.022.
[19] L. Mochalov, et al., Optical emission of two-dimensional arsenic sulfide prepared by plasma, Superlattice. Microst. 114 (Feb. 2018) 305–313, https://doi.org/10.1016/J.SPMI.2017.12.052.
[20] A. Nezhdanov, et al., Impact of composition and ex-situ laser irradiation on the structure and optical properties of as-S-based films synthesized by PECVD, Opt. Mater. (Amst.) 96 (2019), https://doi.org/10.1016/j.optmat.2019.109292, 109292.
[21] J.A. Burunkova, G. Alkhalil, A.V. Veniaminov, I. Csarnovics, S. Molnar, S. Kokenyesi, Arsenic trisulfide-doped silica-based porous glass, Opt. Laser Technol. 147 (2022), 107658, https://doi.org/10.1016/j.optlastec.2021.107658.
[22] O. Kondrat, R. Holomb, A. Csik, V. Takáts, M. Veres, V. Mitsa, Coherent light photo-modification, mass transport effect, and surface relief formation in AsxS100-x Nanolayers: absorption edge, XPS, and Raman spectroscopy combined with Profilometry study, Nanoscale Res. Lett. 12 (1) (Dec. 2017), https://doi.org/10.1186/S11671-017-1918-Y.
[23] H. Fritzsche, J. Tauc, Amorphous and Liquid Semiconductors, Plenum Press, 1974, p. 254.
[24] S.N. Yannopoulos, Structure and photo-induced effects in elemental chalcogens: a review on Raman scattering, J. Mater. Sci. Mater. Electron. 31 (10) (2020) 7565–7595, https://doi.org/10.1007/s10854-020-03310-0.
[25] M. Frumar, A.P. Firth, A.E. Owen, Reversible photodarkening and structural changes in As2S3 thin films, Philos. Mag. B 50 (4) (1984) 463–475, https://doi.org/10.1080/13642818408238871.
[26] R. Holomb, et al., Gold nanoparticle assisted synthesis and characterization of as–S crystallites: scanning electron microscopy, X-ray diffraction, energy-dispersive X-ray and Raman spectroscopy combined with DFT calculations, J. Alloys Compd. 894 (2022), 162467, https://doi.org/10.1016/j.jallcom.2021.162467.
[27] M. Ganaie, M. Zulfequar, M. Ganaie, M. Zulfequar, Study of morphological, electrical and optical behaviour of amorphous chalcogenide semiconductor, in: Advances in Condensed-Matter and Materials Physics - Rudimentary Research to Topical Technology, Jan. 2020, https://doi.org/10.5772/INTECHOPEN.90512.
[28] A.H. Kuptsov, G.N. Zhizhin, Fourier-KR and Fourier-IR Spectra of Polymers, 2013, p. 696.
[29] B. Eckert, R. Steudel, Molecular Spectra of Sulfur Molecules and Solid Sulfur Allotropes, Feb. 2003, pp. 31–98, https://doi.org/10.1007/B13181.
[30] C.M. Finnie, X. Li, P.W. Bohn, Production and evolution of composition, morphology, and luminescence of microcrystalline arsenic oxides produced during the anodic processing of (100) GaAs, J. Appl. Phys. 86 (9) (Oct. 1999) 4997, https://doi.org/10.1063/1.371470.
[31] J.Z. Wu, et al., Fluorescent Realgar Quantum Dots: New Life for an Old Drug, Jan. 2016, https://doi.org/10.1142/S1793292016500053 vol. 11, no. 1.
[32] J. Wang, et al., Arsenic(II) sulfide quantum dots prepared by a wet process from its bulk, J. Am. Chem. Soc. 130 (35) (Sep. 2008) 11596–11597, https://doi.org/10.1021/JA804436W/SUPPL_FILE/JA804436W_SI_001.PDF.
[33] D. Usanov, et al., Some insights into the mechanism of photoluminescence of as-S-based films synthesized by PECVD, J. Non-Cryst. Solids 513 (Jun. 2019) 120–124, https://doi.org/10.1016/J.JNONCRYSOL.2019.03.015.
[34] A. Kovalskiy, M. Vlcek, K. Palka, R. Golovchak, H. Jain, Wavelength dependence of Photostructural transformations in As2S3 thin films, Phys. Procedia 44 (2013) 75–81, https://doi.org/10.1016/j.phpro.2013.04.010.